Security-Constrained Transmission Topology Control MILP Formulation Using Sensitivity Factors

Pablo A. Ruiz, *Member, IEEE,* Evgeniy A. Goldis, Aleksandr M. Rudkevich, *Member, IEEE,*
Michael C. Caramanis, *Member, IEEE,* C. Russ Philbrick, *Senior Member, IEEE,* and
Justin M. Foster, *Member, IEEE*

Abstract—A transmission topology control (TC) framework for production cost reduction based on a shift factor (SF) representation of line flows is proposed. The framework can model topology changes endogenously while maintaining linearity in the overall Mixed Integer Linear Programming (MILP) formulation of the problem. In large power systems it is standard practice to optimize operations considering few but representative contingency constraints. Under these conditions and when tractably small switchable sets are analyzed, the shift factor framework has significant computational advantages compared to the standard $B\theta$ alternative used so far in TC research. These claims are supported and elaborated by numerical results on full models of PJM with over 13,000 buses. We finally present analytical investigations on locational marginal price (LMP) computation in our shift factor TC framework and their relation to LMPs computed for problems without TC. Also, we discuss practical implementation choices such as sufficient conditions on lower bounds that allow selection of large numbers employed in the MILP formulation.

Nomenclature

Scalars are indicated by lower case italic, vectors by lower case bold, matrices by upper case bold, and sets by upper case script characters, indexed appropriately. Upper limits are indicated by an over-bar, and lower limits by an under-bar. Optimal solutions of the problem without topology control are denoted by an asterisk. Sensitivities are indicated with Greek characters.

Indices

m, n	Buses.
k, ℓ	Lines.
i_ℓ	*From* bus of line ℓ.
j_ℓ	*To* bus of line ℓ.
τ	Contingency topology.

Sets and Functions

$\mathcal{L}_{n+}$	Branches whose *to* node is n.
$\mathcal{L}_{n-}$	Branches whose *from* node is n.
$\mathcal{S}$	Switchable branches.
$\mathcal{M}$	Duples $\{\ell, \tau\}$ where branch ℓ is monitored under contingency τ, and branch ℓ is not switchable.

Parameters and Variables for Contingency Topology τ

$b_{\ell\tau}$	Branch ℓ susceptance under contingency τ.
$f_{\ell\tau}$	Branch ℓ flow under τ.
$\underline{f}_{\ell\tau}, \overline{f}_{\ell\tau}$	Transmission limits of branch ℓ under τ.
$\theta_{n\tau}$	Bus n voltage angle under τ.
$v_{\ell\tau}$	Flow-cancelling transaction for branch ℓ under τ.
$\mathbf{v}_\tau$	Vector of flow-cancelling transactions under τ.
$\psi_{\ell\tau}^m$	Shift factor for line ℓ, bus m under τ.
$\phi_{\ell\tau}^{mn}$	PTDF of line ℓ for a transfer from m to n under τ.
$o_{\ell\tau}^k$	LODF of line ℓ for the outage of line k under τ.
$\mathbf{\Phi}_\tau^{\mathcal{SS}}$	PTDF matrix of switchable lines for transfer between switchable line terminals under τ.

Other Parameters and Variables

$\mathbf{1}$	Vector of ones.
$\mathbf{I}$	Identity matrix.
b_ℓ	Susceptance of branch ℓ.
z_ℓ	State of branch ℓ (decision variable).
z_ℓ^0	Initial state of branch ℓ.
c_n^p	Generation variable cost at bus n.
c_ℓ^z	Branch ℓ switching cost.
p_n	Generation at bus n.
$\underline{p}_n, \overline{p}_n$	Generation limits of unit at bus n.
$\mathbf{p}$	Vector of nodal generation.
l_n	Load at bus n.
$\mathbf{l}$	Vector of nodal loads.
λ	Power balance shadow price.
$\underline{\boldsymbol{\mu}}, \overline{\boldsymbol{\mu}}$	Shadow prices of monitored branch constraints.
$\underline{\boldsymbol{\alpha}}, \overline{\boldsymbol{\alpha}}$	Shadow prices of switchable branch constraints.
$\mathbf{\Psi}^{\mathcal{S}}$	Matrix of shift factors of switchable branches.
$\mathbf{\Psi}^{\mathcal{M}}$	Matrix of shift factors of monitored branch-contingency pairs.
$\mathbf{O}^{\mathcal{MS}}$	LODF matrix of monitored branches for the outage of switchable branches.
M	Sufficiently large number.
N	Number of buses.
G	Number of generators.
T	Number of contingency topologies.
Z	Number of switchable lines.
L	Number of transmission lines.
C	Number of monitored/contingent pairs.

I. INTRODUCTION

POWER flows distribute over an AC network following Kirchoff's laws. As such, flows depend on load profile, generation dispatch and transmission topology, including transmission system characteristics, settings and connectivity status. Currently, few transmission branches[1] have flow control devices. The open/closed state of all other branches is typically considered to be non-controllable in operations decision making, such as economic dispatch (ED). Transmission topology changes tend to be considered as decision process inputs, such as a pre-specified contingency list, or as transmission maintenance schedules, and not as decision variables.[2]

The lack of topology control (TC) application persists in spite of substantial research in the area over the last decades. Corrective control [2]–[4], security enhancements [5], [6] and loss minimization [7], [8] are some examples of past investigations. More recently, topology control has been examined for its potential production cost reduction in ED [9]–[11] and unit commitment (UC) [12]. These cost saving opportunities are very promising, with reasonable projections of quantitative results obtained for large systems [13] suggesting several billion dollars in annual savings in the U.S. alone. Production cost minimization is the focus of this paper.

Computational complexity has been a key barrier to systematic use of TC for production cost minimization. The problem has been formulated as a mixed integer linear program (MILP) using the $B\theta$ representation of power flows under DC assumptions. The MILP may incorporate security constraints by solving explicitly for the voltage angles under each contingency state as part of the optimization problem. This is in contrast to standard security-constrained optimal power flow (SCOPF) implementations (without TC), where contingency flow constraints are modeled using sensitivities (shift factors), not requiring contingency state calculations during the optimization solution [14] (contingency states are calculated during contingency analysis checks of proposed SCOPF solutions). The security-constrained $B\theta$ TC formulation has been used to provide and analyze optimal TC in small systems. While the $B\theta$ formulation preserves the network power flow equations' sparsity, it suffers from a very large size and limited scalability. For example, the problem size does not decrease with a smaller number of lines whose connectivity is controlled, or a smaller monitored/contingency element pair set. Moreover, each contingency modeled requires a full transmission model. As such, the model size explodes with security constraints: the SCOPF model with TC on the IEEE 118-bus test system with $n-1$ security constraints requires 63,000 variables and 200,000 constraints, compared to approximately 500 variables and 1000 constraints in the absence of contingency analysis [11]. This leads to prohibitively slow solution times, with integrality gaps of the SCOPF with TC of about 60% after six days of run time [11]. While there have been significant improvements in MILP

solvers and computer resources since the publication of [11], and while formulations have been improved with the addition of symmetry breaking and anti-islanding constraints [15]–[17], the resulting computation times are still very far from the required times for operational deployment in real systems. For example, a recent publication reports over 50 hours to solve an OPF with TC for the Polish 2383-bus system to optimality [18], *without security constraints*.

To overcome computational tractability issues, heuristic approaches have been developed for the TC problem. Some of these heuristics use the $B\theta$ MILP formulation [11]. While parallel algorithms help to lower computational (wall) time, the reduction in computational effort is not enough for practical applications (e.g., an algorithm to optimize a single line switching with N-1 reliability takes over 30 seconds with 24 cores in a small, 300-bus system [19]). Alternative approaches using sensitivity analysis have been very successful in reducing computational times in SCOPF where dispatch is optimized for a single time period [16], [20], [21]. These approaches have been extended to include AC power flow modeling [22]–[24]. However, the extension of these tractable approaches to multi-interval optimization (e.g., UC) is not trivial. Intertemporal constraints, such as maximum number of breakers that can change state on a given interval and maximum switching frequencies, combined with other constraints such as the total number of breakers that can be open at any point in time, require the topology optimization over a multiple time period horizon.

This paper discusses an alternative MILP formulation of the TC problem, recently introduced in [25], [26], called the *shift factor TC formulation*. This new formulation can be applied in both single and multi-period decision making including SCOPF, security-constrained UC, and longer timeframe problems. Consistent with the usual transmission modeling approach in market management systems, the new formulation uses sensitivities to model transmission flows. Instead of changing branch admittances, open breakers are emulated by the use of *flow-cancelling transactions*, e.g., pairs of injections and withdrawals at the ends of opened lines that drive the total flow through the line *interface* with the rest of the system to zero. Compared to the $B\theta$ MILP formulation, the shift factor TC formulation is compact and dense, and its size decreases as the number of monitored/contingent transmission elements pairs and the number of switchable lines decrease. As such, the formulation is especially useful when few constraints need to be explicitly enforced, as is indeed the case in most systems, and when the switchable branches are few compared to the number of branches in the system.

The paper contributes to the state of the art by (a) comparing the numerical performance of the two MILP TC formulations on a real, very large scale system (13,000-bus historical PJM model) in terms of solution time, size and sparsity statistics, and (b) discussing practical application aspects of the shift factor formulation and TC formulations in general, such as LMP calculation from the shift factor TC formulation, bounds for the sufficient magnitude of the number M used, island detection and switching costs.

The rest of the paper has eight sections. Section II presents

---

[1]In this paper, a transmission branch refers to a facility connecting two buses of the network, such as a line or a transformer.

[2]Exceptions exist, such as *operating guides* which specify topology changes upon the occurrence of contingencies or other pre-specified phenomena [1].

the basic power flow model and notation. Section III provides an overview of the $B\theta$ formulation of TC. Section IV describes the modeling of line openings using flow-cancelling transactions. Section V presents the shift factor TC formulation. Section VI discusses LMP calculation in the shift factor TC formulation, and Section VII deals with practical formulation implementation issues. Section VIII compares the computational performance of the two formulations for the SCOPF with TC. Section IX gives concluding remarks and describes future work.

II. POWER FLOW MODEL

The basic underlying SCOPF modeling assumptions used in the two TC formulations are presented in this section.

Consider a power system in which linearized lossless[3] DC assumptions hold. System buses are denoted by $n = 1, \ldots, N$; bus N is the reference bus, with voltage angle 0. Each branch $\ell = 1, \ldots, L$ connects an ordered pair of buses (i_ℓ, j_ℓ), with the convention that the flow direction of branch ℓ is *from* bus i_ℓ and *to* bus j_ℓ. Each branch ℓ is assumed to be closed initially, and is assumed to have non-zero, finite reactance and zero resistance, leading to a non-zero, finite susceptance b_ℓ.

At any point in time, some branches may be disconnected (open), for example due to the occurrence of a contingency. The resulting transmission topology τ is characterized by the zero value of line susceptance $b_{\ell\tau}$ for each open branch ℓ in τ. Generation and load are assumed to be independent of the topology, although they need not be (e.g., under corrective control).

The flow on line ℓ under contingency τ is given by

$$f_{\ell\tau} = b_{\ell\tau} \left(\theta_{j_\ell \tau} - \theta_{i_\ell \tau} \right), \tag{1}$$

where $\theta_{j_\ell \tau}$ is the voltage angle of node j_ℓ under topology τ. Alternatively, the power flow can be expressed as an explicit function of the loads and generation,

$$f_{\ell\tau} = \sum_n \psi_{\ell\tau}^n \left(p_n - l_n \right). \tag{2}$$

The *injection shift factor* $\psi_{\ell\tau}^n$ gives the variation in flow of line ℓ under topology τ due to changes in the nodal injection at bus n [14], with the reference bus assumed to ensure the real power balance. Shift factors are a function of transmission facilties' susceptances and the topology (τ).

The *power transfer distribution factor* $\phi_{\ell\tau}^{mn}$, or *PTDF*, gives the sensitivity of the flow on line ℓ with respect to a unit of power transfered from bus m to bus n under topology τ, and can be expressed in terms of shift factors as [14]

$$\phi_{\ell\tau}^{mn} = \psi_{\ell\tau}^m - \psi_{\ell\tau}^n. \tag{3}$$

The *line outage distribution factor* o_ℓ^k, or *LODF*, gives the sensitivity of line ℓ flow with respect to a reduction in the line k flow, $o_\ell^k = -\partial f_\ell / \partial f_k$. The LODF o_ℓ^k is given by [14]

$$o_k^k = -1, \tag{4}$$

$$o_\ell^k = \frac{\phi_\ell^{i_k j_k}}{1 - \phi_k^{i_k j_k}}, \ell \neq k, \phi_k^{i_k j_k} \neq 1, \tag{5}$$

[3] The extension to incorporate losses is provided in [26]

and is not defined for all $\ell \neq k$ if $\phi_k^{i_k j_k} = 1$, because the outage of such lines creates islands [27], which require generation re-dispatch and/or load shedding. The PTDF $\phi_k^{i_k j_k}$ of line k for transactions from its *from* bus to its *to* bus is positive and between 0 and 1,

$$1 \geq \phi_k^{i_k j_k} > 0. \tag{6}$$

III. $B\theta$ TOPOLOGY CONTROL FORMULATION

The typical MILP formulations of topology control problems model transmission flows using (1), i.e., explicitly keeping the susceptances as inputs and voltage angles as decision variables [10]–[12], hence the name $B\theta$ formulation. The supply-demand balance is enforced at the nodal level. This model is used because the linear inclusion of binary variables associated with the connection or disconnection of branches is more intuitive in it than it is with the shift factor power flow model, which has a nonlinear dependence on susceptances and connectivity (equation (2)).

In the remainder of this paper, τ will indicate the forced topology changes due to a contingency. The selected topology changes due to controlled actions are specified by the $0/1$ (open/closed) status of each *switchable* branch ℓ, indicated by z_ℓ. Together, τ and the set of z_ℓ define a transmission topology.

Without loss of generality, assume there is at most one generator per bus, and it has constant marginal costs. The SCOPF with TC minimizes generator and switching costs (7) to serve load subject to physical constraints such as generator (8) and line (9) limits. The incorporation of TC requires the addition of a binary variable (13), which renders the problem an MILP. This variable represents line status, taking the value of 1 when the line is closed and 0 when open. The power balance at each bus is enforced by (10). In addition, (11) and (12) define flows as a function of voltage angles, where M is a sufficiently large number. The line susceptance $b_{\ell\tau}$ takes the value of 0 when contingency τ outages line ℓ, and the value of b_ℓ otherwise. Note that this formulation computes angles for all buses and flows on all lines for each contingency τ of a pre-specified contingency list.

$$\mathcal{C} = \min_{\mathbf{p}, \boldsymbol{\theta}, \mathbf{f}, \mathbf{z}} \sum_n c_n^p p_n + \sum_\ell c_\ell^z \left(z_\ell - z_\ell^0 \right) \tag{7}$$

$$\text{s.t.} \quad \underline{p}_n \leq p_n \leq \overline{p}_n, \quad \forall n \tag{8}$$

$$\underline{f}_{\ell\tau} z_\ell \leq f_{\ell\tau} z_\ell \leq \overline{f}_{\ell\tau} z_\ell, \quad \forall \ell, \tau \tag{9}$$

$$\sum_{\ell \in \mathcal{L}_{n+}} f_{\ell\tau} - \sum_{\ell \in \mathcal{L}_{n-}} f_{\ell\tau} + p_n = l_n, \quad \forall n, \tau \tag{10}$$

$$b_{\ell\tau} \left(\theta_{j_\ell \tau} - \theta_{i_\ell \tau} \right) + (1 - z_\ell) M \geq f_{\ell\tau}, \quad \forall \ell, \tau \tag{11}$$

$$b_{\ell\tau} \left(\theta_{j_\ell \tau} - \theta_{i_\ell \tau} \right) - (1 - z_\ell) M \leq f_{\ell\tau}, \quad \forall \ell, \tau \tag{12}$$

$$z_\ell \in \{0, 1\}, \quad \forall \ell \tag{13}$$

In the remainder of the paper, problem (7)-(13) is referred to as the $B\theta$ *TC formulation*. Let the number of generators be G, the number of contingencies be T and the number of switchable lines be Z. The $B\theta$ TC formulation has approximately $G + (N - 1)T + LT + Z$ decision variables and $2G + 4LT + NT + Z$ constraints. The number of non-zero

problem entries is $o\big((L+N)T\big)$. As such, the problem dimension is essentially insensitive to the number of switchable lines and monitored transmission constraints, in contrast to the formulation to be introduced next.

IV. FLOW-CANCELLING TRANSACTIONS

The direct approach to modeling a branch outage is to set the branch susceptance to zero or to remove it from the susceptance matrix, as the $B\theta$ formulation does. An alternative approach is to maintain the original topology and susceptances, but to apply a power transfer across the outaged branch that results in the same changes in the remaining branch flows, so that from the point of view of the rest of the system, the branch is outaged.

The modeling approach of representing outages as a flow-cancelling transaction is widely known, for example, as a tool to derive LODFs [14]. This approach is valid as long as no islanding results from the outages. Consider first the derivation of a flow-cancelling transaction for a single line. To model the outage of line k, which does not island the system, let i'_k and j'_k be infinitely close to the terminal buses i_k and j_k along line k (Fig. 1). Let there be a transaction from i'_k to j'_k whose magnitude $v_{k\tau}$ is such that the impact of the trasaction on the rest of the system is equivalent to the opening of line k. To meet this condition, the flow-cancelling transaction must make the flow on the interface between the rest of the system and line k, i.e., each of the infinitesimaly short lines i'_k to i_k and j'_k to j_k, to be zero. Using the PTDF definition,

$$f_{k\tau} - \left(1 - \phi_{k\tau}^{i'_k j'_k}\right) v_{k\tau} = 0. \tag{14}$$

Hence,

$$v_{k\tau} = \frac{f_{k\tau}}{1 - \phi_{k\tau}^{i'_k j'_k}} = \frac{f_{k\tau}}{1 - \phi_{k\tau}^{i_k j_k}}. \tag{15}$$

The flow-cancelling transaction is well defined, since $\phi_{k\tau}^{i_k j_k} \neq 1$ when the non-islanding assumption holds [27].

The vector of flow-cancelling transactions that model the outage of a (non-islanding) set $\mathcal{S}$ of lines can be obtained by applying the principle of superposition, i.e., by enforcing condition (14) for all lines in the set [28],

$$f_{\tau\ell} - v_{\ell\tau} + \sum_{k \in \mathcal{S}} \phi_{\ell\tau}^{i_k j_k} v_{k\tau} = 0, \quad \forall \ell \in \mathcal{S}. \tag{16}$$

The PTDFs in (16) are those for transactions between the terminal points of lines in $\mathcal{S}$, with respect to the flows of lines in $\mathcal{S}$. We term the matrix $\boldsymbol{\Phi}_\tau^{\mathcal{S}\mathcal{S}}$ containing these PTDF as the *self-PTDF matrix* of set $\mathcal{S}$. As long as there is no islanding, (16) has a unique solution $\mathbf{v}_\tau$. Under islanding conditions, network flows are not well-defined without additional equations enforcing power balance in each island.[4]

The utilization of flow-cancelling transactions in our new MILP topology control formulation is discussed below.

---

[4]If $\mathcal{S}$ is islanding, there are infinite $\mathbf{v}_\tau$ that meet (16) but these flow-cancelling transactions may not represent islanded operation.
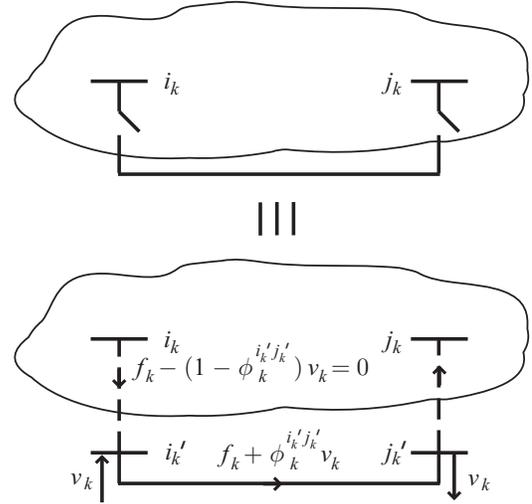

Fig. 1. Opening line k (top) is equivalent from the point of view of the rest of the system as inserting a flow-cancelling transaction at virtual buses i'_k and j'_k, infinitely close to i_k and j_k, respectively, and along line k (bottom).

V. A COMPACT TOPOLOGY CONTROL FORMULATION

For a given contingency τ there are typically only a few transmission elements that are likely to reach their limiting flow and therefore need to be monitored. For example, consider parallel lines k and k', and assume that all transmission constraints are met in the base topology. It is frequently the case that ensuring that line k does not overload after the outage of parallel line k' is sufficient to ensure that no other transmission constraint violations will occur with the outage of line k. In other words, all other constraints in (9) would not bind under the outage of line k. Even in the base, no-contingency topology, the number of limiting transmission branches in actual systems is typically a very small fraction of the total number of lines and transformers.[5]

To reduce the problem size by modeling only significant constraints, the SCOPF problem is usually formulated using (2) instead of (1). This allows the substitution of (10) by a single power balance equation,

$$\sum_n (p_n - l_n) = 0. \tag{17}$$

Moreover, all equations/rows in (2) that are not related to monitored branches in each contingency topology are eliminated. While the resulting problem is significantly smaller, both in terms of constraints and variables (e.g., voltage angles are no longer modeled explicitly), the remaining equations are more dense since shift factors form a dense matrix while the susceptance terms in (1) form a very sparse matrix. Still, due to the very small number of monitored constraints, reduced size favors the dense formulation which in practice solves faster.

For each contingency τ, let $v_{\ell\tau}$ be the flow-cancelling transaction to model the state of switchable line ℓ. For the closed switchable lines, (2) needs to be enforced with appropriate

---

[5]For example, the number of constraints binding in PJM real-time markets is usually less than 10, although PJM monitors over 6500 transmission branches and models over 6000 contingencies in its contingency analysis applications [29].

limits, similar to (9). For the open switchable lines, (16) needs to be enforced in addition to (2). This is achieved through additional constraints,

$$\underline{f}_{\tau,\ell} z_\ell \leq \sum_n \psi_{\ell\tau}^n (p_n - l_n) - v_{\ell\tau}$$
$$+ \sum_{k\in\mathcal{S}} \phi_{\ell\tau}^{i_k j_k} v_{k\tau} \leq \overline{f}_{\tau,\ell} z_\ell, \qquad \forall \ell \in \mathcal{S}, \tau \quad (18)$$

$$-M(1 - z_\ell) \leq v_{\ell\tau} \leq M(1 - z_\ell), \quad \forall \ell \in \mathcal{S}, \tau. \quad (19)$$

For a sufficiently large M, constraints (19) force the flow-cancelling transactions to be 0 for all closed lines, while allowing them to be unrestricted for all open lines.

Note that the flow-cancelling transaction $v_{\ell\tau}$ is a function of the contingency τ as well as the selected state $\mathbf{z}$ of switchable branches, in the same way that angles in (11-12) depend on $\mathbf{z}$ and τ. That is, each flow-cancelling transaction is represented by a set of magnitudes: one for the base case and one for each contingency, and all of these magnitudes depend on the selected $\mathbf{z}$. Opening a branch will require different flow-cancelling injection/withdrawal pairs under different topologies induced by the outage of contingency branches.

Let $\mathcal{M}$ be the set of duples $\{\ell, \tau\}$ where branch ℓ is monitored under contingency τ, and branch ℓ is not switchable. In the remainder of the paper, a monitored branch means a monitored branch that is not switchable, as all switchable lines are explicitly included in the problem formulation, and thus monitored. For monitored branches, the flow constraints incorporate the impacts of flow-cancelling transactions for switchable lines, and are given by

$$\underline{f}_{\tau,\ell} z_\ell \leq \sum_n \psi_{\ell\tau}^n (p_n - l_n)$$
$$+ \sum_{k\in\mathcal{S}} \phi_{\ell\tau}^{i_k j_k} v_{k\tau} \leq \overline{f}_{\tau,\ell} z_\ell, \quad \forall \{\ell, \tau\} \in \mathcal{M}. \quad (20)$$

The resulting formulation of the SCOPF with TC is

$$\mathcal{C} = \min_{\mathbf{p}, \boldsymbol{\theta}, \mathbf{f}, \mathbf{z}} \sum_n c_n^p p_n + \sum_\ell c_\ell^z (z_\ell - z_\ell^0) \quad (21)$$

$$\text{s.t.} \quad \sum_n (p_n - l_n) = 0, \quad (22)$$

$$\underline{p}_n \leq p_n \leq \overline{p}_n, \quad \forall n \quad (23)$$

$$\underline{f}_{\tau,\ell} \leq \sum_n \psi_{\ell\tau}^n (p_n - l_n)$$
$$+ \sum_{k\in\mathcal{S}} \phi_{\ell\tau}^{i_k j_k} v_{k\tau} \leq \overline{f}_{\tau,\ell}, \quad \forall \{\ell, \tau\} \in \mathcal{M} \quad (24)$$

$$\underline{f}_{\tau,\ell} z_\ell \leq \sum_n \psi_{\ell\tau}^n (p_n - l_n) - v_{\ell\tau}$$
$$+ \sum_{k\in\mathcal{S}} \phi_{\ell\tau}^{i_k j_k} v_{k\tau} \leq \overline{f}_{\tau,\ell} z_\ell, \quad \forall \ell \in \mathcal{S}, \tau \quad (25)$$

$$-M(1 - z_\ell) \leq v_{\ell\tau} \leq M(1 - z_\ell), \quad \forall \ell \in \mathcal{S}, \tau, \quad (26)$$
$$z_\ell \in \{0, 1\}, \quad \forall \ell \quad (27)$$

Problem (21)-(27), referred to as the *shift factor TC formulation*, yields the same optimal solution as the $B\theta$ formulation as long as the transmission constraints that bind in the

$B\theta$ formulation are modeled in the shift factor formulation. However, problem size and complexity are quite different. The shift factor TC formulation has $G + TZ + Z$ decision variables and $1 + 2G + 2C + 4TZ + Z$ constraints, where C is the number of monitored/contingency pairs. The number of non-zero problem entries is $o\big((N + Z)(C/T + Z)T\big)$. If the number of switchable branches and monitored/contingency pairs are relatively small, the shift factor formulation is significantly smaller than the $B\theta$ formulation in every sense. As the number of switchable, monitored and contingency lines becomes sufficiently large, the number of non-zero elements in the shift factor formulation becomes larger than in the $B\theta$ TC formulation, although the number of constraints always remains smaller in the shift factor formulation, as there is a single power balance equation.

VI. LOCATIONAL MARGINAL PRICES

While the shift factor TC formulation is consistent with standard SCOPF formulations used in nodal markets, there are additional constraints (25) that require modifications to the standard locational marginal price (LMP) expressions used in the markets. This section determines these modifications, and shows how the LMPs in the shift factor TC formulation can be equivalently expressed in the usual form as the LMPs of a SCOPF (without TC) for the optimal $\mathbf{z}$.

By definition, the LMPs for the SCOPF with TC (21)-(27) equal the derivative of the Lagrangian with respect to a change in nodal load [30]. In this section, we use vector notation for brevity and clarity. Let the vectors of shadow prices associated with constraints (22), (24), and (25) be denoted by λ, $\underline{\boldsymbol{\mu}}$ and $\overline{\boldsymbol{\mu}}$, and $\underline{\boldsymbol{\alpha}}$ and $\overline{\boldsymbol{\alpha}}$, respectively. Using these shadow prices, the nodal prices $\boldsymbol{\pi}$ under the shift factor TC formulation are given by

$$\boldsymbol{\pi} = -\big(\lambda \mathbf{1} + \boldsymbol{\Psi}^{\mathcal{M}'}(\overline{\boldsymbol{\mu}} - \underline{\boldsymbol{\mu}}) + \boldsymbol{\Psi}^{\mathcal{S}'}(\overline{\boldsymbol{\alpha}} - \underline{\boldsymbol{\alpha}})\big), \quad (28)$$

where $\boldsymbol{\Psi}^{\mathcal{S}}$ and $\boldsymbol{\Psi}^{\mathcal{M}}$ are matrices that consist of the collection of $\boldsymbol{\Psi}_\tau^{\mathcal{S}}$ and $\boldsymbol{\Psi}_\tau^{\mathcal{M}}$, for all contingencies τ, respectively. Also, the shadow prices $\underline{\boldsymbol{\mu}}$, $\overline{\boldsymbol{\mu}}$, $\underline{\boldsymbol{\alpha}}$ and $\overline{\boldsymbol{\alpha}}$ have as elements the corresponding shadow prices for each contingency.

To gain intuition with respect to (28), consider the optimal (base) topology derived from the solution $\mathbf{z} = \mathbf{z}^*$ of (21)-(27). Also, relabel ex-post any switchable lines which remain closed in the optimal topology as monitored (including relabeling as elements of $\underline{\boldsymbol{\mu}}$ and $\overline{\boldsymbol{\mu}}$ the terms of $\underline{\boldsymbol{\alpha}}$ and $\overline{\boldsymbol{\alpha}}$, respectively, associated to these closed switchable lines). The shift factor matrix for the optimal topology $\mathbf{z}^*$ is given in [14] as

$$\boldsymbol{\Psi}^{\mathcal{M}*} = \boldsymbol{\Psi}^{\mathcal{M}} + \mathbf{O}^{\mathcal{M}\mathcal{S}} \boldsymbol{\Psi}^{\mathcal{S}}, \quad (29)$$

where $\mathbf{O}^{\mathcal{M}\mathcal{S}}$ is the LODF matrix indicating the impact of lines openings on monitored lines for each contingency. In addition, the LMPs for the optimal topology $\mathbf{z}^*$ are defined in the standard manner (see [14]), as

$$\boldsymbol{\pi}^* = -\big(\lambda^* \mathbf{1} + \boldsymbol{\Psi}^{\mathcal{M}*'}(\overline{\boldsymbol{\mu}}^* - \underline{\boldsymbol{\mu}}^*)\big). \quad (30)$$

Since the SCOPFs with TC and without TC for the optimal topology $\mathbf{z}^*$ yield equivalent solutions, the LMPs (31) and

shadow prices associated with flow limits on transmission elements and flowgates (32) must be equivalent:

$$\boldsymbol{\pi} = \boldsymbol{\pi}^*, \tag{31}$$

$$\boldsymbol{\mu} = \boldsymbol{\mu}^*. \tag{32}$$

Substituting (28) and (30) into (31), and cancelling the energy component yields,

$$\boldsymbol{\Psi}^{\mathcal{M}'}(\overline{\boldsymbol{\mu}} - \underline{\boldsymbol{\mu}}) + \boldsymbol{\Psi}^{\mathcal{S}'}(\overline{\boldsymbol{\alpha}} - \underline{\boldsymbol{\alpha}}) = \boldsymbol{\Psi}^{\mathcal{M}'*}(\overline{\boldsymbol{\mu}}^* - \underline{\boldsymbol{\mu}}^*). \tag{33}$$

Furthermore, substituting (29) and (32) and appropriately cancelling like terms yields,

$$\overline{\boldsymbol{\alpha}} - \underline{\boldsymbol{\alpha}} = \mathbf{O}^{\mathcal{MS}'}(\overline{\boldsymbol{\mu}} - \underline{\boldsymbol{\mu}}). \tag{34}$$

Thus, based on [16], the shadow prices $\overline{\boldsymbol{\alpha}} - \underline{\boldsymbol{\alpha}}$ are interpreted as (minus) the total derivative of the generation costs with respect to reducing flow on the (opened) switchable lines.

Finally, by substituting (34) into (28) we see that the LMP (28) derived from the SCOPF with TC can be expressed in the standard form as

$$\boldsymbol{\pi} = -\left(\lambda \mathbf{1} + (\boldsymbol{\Psi}^{\mathcal{M}} + \mathbf{O}^{\mathcal{MS}}\boldsymbol{\Psi}^{\mathcal{S}})'(\overline{\boldsymbol{\mu}} - \underline{\boldsymbol{\mu}})\right). \tag{35}$$

VII. FORMULATION IMPLEMENTATION ASPECTS

This section discusses issues of practical importance related to the implementation of TC formulation – switching costs, bounds on M and a method for fast islanding conditions detection which facilitate the implementation of the shift factor TC formulation.

Switching costs c_ℓ^z are included in the objective functions (7) and (21) for completeness, although they need not be used. In general, increased frequency of breaker operation increases the cost of circuit breaker maintenance. However, these cost are negligible compared to congestion cost benefits provided by topology control. For example, the overhaul cost of a 72.5 kV SF_6 breaker is in the \$15,000-\$20,000 range [31]. The overhaul frequency is once every 2000-5000 operations depending on the type of breaker, and it may be deferred with X-ray diagnostics. Thus, the switching costs are less than \$10/switching operation cycle, and could be as low as a few dollars. Switching costs may also be used for computational reasons, to discourage solutions with spurious switchings (e.g., switching operations that do not add value but do not lead to increased congestion either), or to filter out switching operations that do not provide significant benefits.

In the shift factor TC formulation, the only parameter that is left without a precise value is M, defined simply as a *sufficiently large number*. From (15), $v_{k\tau} = f_k + \phi_{k\tau}^{m'n'} v_{k\tau}$. Thus, the value of the flow-cancelling transaction is equal to the flow on line k when the angle difference between its terminals is equal to the angle difference that occurs when the line is opened (for an illustration, refer to Fig. 1). Hence, if line k is open, for any contingency topology τ the following holds (as long as there is no islanding):

$$v_{k\tau} = b_k \left(\theta_{j_k\tau} - \theta_{i_k\tau}\right). \tag{36}$$

From (36), we can see that M can be bounded by the maximum potential value of the product of the line susceptance and angle difference. Indeed,

$$\max_{k,\tau}(v_{k\tau}) = \max_{k,\tau}\left(b_k\left(\theta_{j_k\tau} - \theta_{i_k\tau}\right)\right) \tag{37}$$

$$\leq \max_k(b_k)\max_{k,\tau}\left(\theta_{j_k\tau} - \theta_{i_k\tau}\right) \tag{38}$$

$$= M. \tag{39}$$

Note that this same bound is applicable for setting the M value in the $B\theta$ formulation, since $f_k = 0$ when $z_k = 0$, so that the M value from (39) ensures that (11) and (12) are met.

Under normal conditions, islanding operation is undesirable, leading to incorrect description of constraints and possibly reliability concerns. As such, fast islanding detection, both for the normal state and for all contingency states, is important when change of the transmission topology is contemplated. As in the previous section, let us relabel ex-post any switchable lines which remain closed in the optimal topology as monitored. Using results in [27], islanding can be detected quickly by evaluating the singularity of matrices $\left(\boldsymbol{\Phi}_\tau^{\mathcal{SS}} - \mathbf{I}\right)$ for all contingencies τ. Note that these matrices are already available. Also, while the number of such matrices could be non-trivial, the matrices are relatively small, with size equal to the number of branches opened in the optimal topology. Finally, the singularity evaluations can be done in parallel, further speeding the analysis.

VIII. NUMERICAL EXPERIENCE ON A LARGE SYSTEM

The shift factor TC formulation was previously compared against the $B\theta$ TC formulation using the IEEE 118-bus test system in [25]. Analysis of a range of switchable sets, varying from no switchable lines to 24 switchable lines (i.e., over 12% of the 194 lines in the system) yielded that the shift factor TC formulation has lower computational times for all switchable set sizes analyzed. However, the computational savings were more significant for smaller switchable sets, as expected due to the dependence of the shift factor formulation size on the cardinality of the switchable set.

In this paper we compare the performance of both formulations using a large, real system model. The model represents in detail the state of PJM's footprint and its neighboring areas on June 23, 2010 at 8:30 am. This interval was selected based on the average results obtained on it when applying tractable TC policies such as those in [16]. The underlying topology, load, losses, interchange and unit commitment is as archived by the PJM EMS for that 5-minute interval. Generation economic and constraint data are from the PJM real-time market for the simulated day. The model has 857 dispatchable PJM generators, 13,436 buses and 18,415 branches.

Thirty contingency constraints and 156 no-contingency constraints were enforced. The 30 contingency constraints include 20 different transmission contingencies (some constraints share the same contingency). The contingency constraint limits are based on emergency ratings of the corresponding monitored transmission branch. These constraints are based on the monitored constraints in the PJM real-time markets during the week of June 20-26, 2010.

Both TC formulations were implemented in AIMMS 3.12 and CPLEX 12.5 was used to solve the optimization programs. Simulations were run on a 64-bit workstation with two 2.93 GHz Intel Xeon processors (8 cores total) and 24 GB of RAM. The convergence criterion was an optimality gap tolerance of 0.05%. A value of 5000 was used for M in both formulations (as discussed in Section VII, the M values in both formulations are equivalent). Unless indicated explicitly, the same default CPLEX settings were used to solve problems with both formulations (the only difference is for the cases where we tested the barrier method for the $B\theta$ formulation). A time limit of 1 hour was used for all simulations.

The TC formulations implemented and tested include two types of constraints not detailed in the previous sections for simplicity. We added connectivity constraints that ensure that each generator and load bus is connected by at least two lines, and symmetry-breaking constraints that provide a preferred ordering for each group of identical parallel lines.

Two sets of cases were evaluated, with and without contingency constraints, to illustrate the significant impacts of contingency constraints on solution times. First, each case was solved without TC variables (e.g., standard SCOPF) to provide benchmarks. Then, TC variables were included and both formulations were compared in terms of solution times and topology change statistics. To produce statistically meaningful results, each set was run for 20 cases constructed by taking random samples of fuel prices and wind availabilities. Additionally, for the $B\theta$ formulation we evaluated the default Dual Simplex method as well as the Barrier method available in CPLEX for solving the LP subproblems of the MIP.

Table I sumarizes solution time statistics across the 20 samples, reported in seconds, for the cases without TC (using the CPLEX LP solver). The abbreviation DS refers to the Dual Simplex method used by default in CPLEX and B refers to the Barrier method.

TABLE I
SOLUTION TIME STATISTICS – WITHOUT TC [S]

	Without Contingencies			With Contingencies		
	$B\theta$ - DS	$B\theta$ - B	Ψ	$B\theta$ - DS	$B\theta$ - B	Ψ
Avg	0.65	0.54	0.12	37.28	80.24	0.67
Min	0.42	0.50	0.06	14.49	26.80	0.64
Max	0.91	0.62	0.14	74.37	541.09	0.70
Std Dev	0.13	0.03	0.02	14.31	129.69	0.02

As seen in Table I, the shift factor (Ψ) formulation solves significantly faster than the $B\theta$ formulation, especially when contingency constraints are enforced, when the average Ψ formulation solution time is over 500 times faster. It appears that despite the sparsity benefits of the $B\theta$ formulation, the significant increase in variables and constraints shown in Table II results in much slower solution times. Also of note is the consistency in solution times observed for the Ψ formulation: the standard deviation of the solution time is about 3% of the average solution time, where for the $B\theta$ formulation the ratio is of over 38%. It is these advantages in compactness and solution time magnitude and consistency that make the Ψ models of transmission constraints the preferred choice for industrial decision support tools used in very large systems.

For the $B\theta$ formulation, the Barrier method performs better for the small case without contingencies but for the large case with contingencies it becomes less stable as shown by the high standard deviation value. Specifically, for two samples the solution times were significantly larger than for all other samples (351 and 541 seconds respectively). If these times are excluded from the statistics of Table I, the minimum time and standard deviation is still higher than for the Dual Simplex method but the average and max times are very similar.

TABLE II
CONSTRAINT & VARIABLE STATISTICS – NO TC WITH CONTINGENCIES

Variables	$B\theta$	Ψ
Flow	386, 715	0
Voltage Angle	282, 156	0
Generator	857	857
Total	669, 728	857
Constraints	$B\theta$	Ψ
Flow Limits (2x)	586	586
Kirchhoff	386, 715	0
Nodal Balance	282, 156	1
Generation Limits (2x)	857	857
Total	671, 757	2, 886
Matrix Density (%)	0.0036%	21.28%

TABLE III
TOPOLOGY CHANGE STATISTICS WITH 20 SWITCHABLE BRANCHES

	Without Contingencies			With Contingencies		
Openings	$B\theta$ - DS	$B\theta$ - B	Ψ	$B\theta$ - DS	$B\theta$ - B	Ψ
Median	4	4	3	6	3	9
Min	2	2	1	0	0	3
Max	12	10	7	20	20	15
Savings	$B\theta$ - DS	$B\theta$ - B	Ψ	$B\theta$ - DS	$B\theta$ - B	Ψ
Prod. Cost (%)	0.6	0.6	0.6	0.2*	0.8*	1.1*
Cong. Cost (%)	4.5	4.5	4.5	2.8*	6.6*	9.6*

* Savings for the $B\theta$ formulation are lower than those of the Ψ formulation because of the lack of convergence within an hour of several scenarios with the $B\theta$ formulation (including all samples with the barrier method).

Next we introduce 20 switchable branches into both formulations. The switchable lines were selected based on the solutions of heuristic approaches using sensitivity metrics [16]. The topology change statistics and the average production cost savings and congestion cost savings are in Table III (congestion cost savings are defined as the production cost savings relative to the cost of congestion without TC). For the case without contingencies, both formulations yielded almost identical savings (they are not identical since we are solving with a 0.5% MIP gap), although the solutions were different, and the Ψ formulation tended to open fewer lines. With the inclusion of contingencies, the $B\theta$ formulation reaches the one hour time limit without converging in 11 out of 20 samples with the dual simplex algorithm, and does not converge within an hour for any sample for the barrier algorithm. Thus, there are very significant differences between the "solutions" provided by the two formulations and by the two solution methods at the end of the hour.

Table IV shows solution time statistics when we introduce TC variables into both formulations. Including the 20 switchable lines in the case with contingencies increases the

average solution time of the $B\theta$ formulation by about 85 times from the OPF without TC, whereas the increase for the Ψ formulation is about 10 times. As a result, the Ψ formulation solves about three orders of magnitude faster than the $B\theta$ formulation. The range of solution times for the Ψ formulation remained relatively tight, with a standard deviation of the solution time of less than 15% of the average time. The Ψ formulation reached the MIP gap tolerance for all cases in a few seconds, where the $B\theta$ formulation did not reach the convergence tolerance within an hour in most samples, as stated before. Hence, the actual average and maximum solution times for converged solutions are higher than those in Table IV for the $B\theta$ formulation. From these results, we conclude that in contrast to the $B\theta$ formulation, the Ψ formulation is practical for large systems when the number of switchable lines and contingency constraints is small.

TABLE IV
SOLUTION TIME STATISTICS – WITH TC [S]

	Without Contingencies			With Contingencies[6]		
	$B\theta$ - DS	$B\theta$ - B	Ψ	$B\theta$ - DS	$B\theta$ - B	Ψ
Avg	26.80	29.24	0.57	3,246	3,672	6.98
Min	2.76	5.12	0.56	1,407	3,605	5.13
Max	107.67	85.72	0.58	3,927	3,939	9.36
Std Dev	30.81	22.20	0.01	685	99	1.01

IX. CONCLUDING REMARKS

We have developed a new MILP-based TC formulation based on shift factors that is consistent with the ED and UC formulations currently used in practice for large systems. In contrast with the widely published $B\theta$ TC formulation, the shift factor TC formulation is compact and scales with the number of decision variables (switchable lines) and transmission constraints (monitored lines and contingencies). While the shift factor formulation is significantly denser than the $B\theta$ formulation, it solves orders of magnitude faster in large systems and for TC problems with a reduced number of switchable lines where the majority of the relevant operational constraints are contingency constraints (as is the case in most practical systems).

Several assumptions used in this paper can be easily relaxed. While lossless DC power flow assumptions were used for ease of presentation, our methodology applies to any linearized power flow assumptions. For example, a linearization gap, or bias, can easily be incorporated. Marginal loss impacts can be incorporated by properly adjusting the sensitivities used, as shown in [26]. Also, it is simple to formulate hybrid TC problems, where the $B\theta$ model is used to fully describe normal operating conditions, and the shift factor model with flow-cancelling transactions are used to enforce selected contingency constraints. Multi-period ED and UC can be accommodated. In these problems, constraints on the maximum frequency of switching for a branch or the maximum number of switching operations in a period can be

modeled. Finally the cost of switching can be added in the objective function.

Future work will focus on the development of iterative heuristics using the shift factor formulation, explicit modeling of AC impacts, the incorporation of substation reconfiguration (opening of near zero-impedance branches) as potential TC actions, and the study of dynamic topology control in ED and UC formulations. Also, the shift-factor formulation is promising for application to transmission maintenance scheduling and transmission expansion planning, as well as chronological production cost and reliability simulation with stochastic topology (e.g., due to transmission outages) and resources [32].

REFERENCES

[1] Switching solutions. PJM Interconnection. Accessed Jan 20, 2016. [Online]. Available: http://www.pjm.com/markets-and-operations/etools/oasis/system-information/switching-solutions.aspx

[2] A. Mazi, B. Wollenberg, and M. Hesse, "Corrective control of power system flows by line and bus-bar switching," *IEEE Trans. Power Syst.*, vol. 1, no. 3, pp. 258–264, Aug. 1986.

[3] A. G. Bakirtzis and A. P. S. Meliopoulos, "Incorporation of switching operations in power system corrective control computations," *IEEE Trans. Power Syst.*, vol. 2, no. 3, pp. 669–675, Aug. 1987.

[4] W. Shao and V. Vittal, "Corrective switching algorithm for relieving overloads and voltage violations," *IEEE Trans. Power Syst.*, vol. 20, no. 4, pp. 1877–1885, Nov. 2005.

[5] G. Schnyder and H. Glavitsch, "Security enhancement using an optimal switching power flow," *IEEE Trans. Power Syst.*, vol. 5, no. 2, pp. 674–681, May 1990.

[6] H. Glavitsh, "Power system security enhanced by post-contingency switching and rescheduling," in *Proc. IEEE Power Tech 1993*, Sept. 1993, pp. 16–21.

[7] R. Bacher and H. Glavitsch, "Loss reduction by network switching," *IEEE Trans. Power Syst.*, vol. 3, no. 2, pp. 447–454, May 1988.

[8] S. Fliscounakis, F. Zaoui, G. Simeant, and R. Gonzalez, "Topology influence on loss reduction as a mixed integer linear programming problem," in *Proc. IEEE Power Tech 2007*, July 2007, pp. 1987–1990.

[9] R. O'Neill, R. Baldick, U. Helman, M. Rothkopf, and W. Stewart, "Dispatchable transmission in RTO markets," *IEEE Trans. Power Syst.*, vol. 20, no. 1, pp. 171–179, Feb. 2005.

[10] E. B. Fisher, R. P. O'Neill, and M. C. Ferris, "Optimal transmission switching," *IEEE Trans. Power Syst.*, vol. 23, no. 3, pp. 1346–1355, Aug. 2008.

[11] K. W. Hedman, R. P. O'Neill, E. B. Fisher, and S. S. Oren, "Optimal transmission switching with contingency analysis," *IEEE Trans. Power Syst.*, vol. 23, no. 3, pp. 1577–1586, Aug. 2009.

[12] K. W. Hedman, M. C. Ferris, R. P. O'Neill, E. B. Fisher, and S. S. Oren, "Co-optimization of generation unit commitment and transmission switching with n-1 reliability," *IEEE Trans. Power Syst.*, vol. 25, no. 2, pp. 1052–1063, May 2010.

[13] E. A. Goldis, X. Li, M. C. Caramanis, B. Keshavamurthy, M. Patel, A. M. Rudkevich, and P. A. Ruiz, "Applicability of topology control algorithms (TCA) to a real-size power system," in *Proc. 51th Allerton Conf. on Communications, Control and Computing*, Monticello, IL, Oct. 2013.

[14] B. Wollenberg and A. Wood, *Power Generation, Operation and Control*, 2nd ed. New York, NY: John Wiley, 1996.

[15] J. Ostrowski, J. Wang, and C. Liu, "Exploiting symmetry in transmission lines for transmission switching," *IEEE Trans. Power Syst.*, vol. 27, no. 3, pp. 1708–1709, Aug. 2012.

[16] P. A. Ruiz, J. M. Foster, A. Rudkevich, and M. C. Caramanis, "Tractable transmission topology control using sensitivity analysis," *IEEE Trans. Power Syst.*, vol. 27, no. 3, pp. 1550–1559, Aug. 2012.

[17] J. Ostrowski, J. Wang, and C. Liu, "Transmission switching with connectivity-ensuring constraints," *IEEE Trans. Power Syst.*, vol. 29, no. 6, pp. 2621–2627, Nov. 2014.

[18] O. Makelä, J. Warrington, M. Morari, and G. Andersson, "Optimal transmission line switching for large-scale power systems using the alternating direction method of multipliers," in *Proc. 18th Power Syst. Comp. Conf.*, Wroclaw, Poland, Aug. 2014.

[6]Even though a max time limit of 3,600 seconds was set, some times are longer because the solver may be in the middle of an internal iteration.

[19] G. Poyrazoglu and H. Oh, "Optimal topology control with physical power flow constraints and N-1 contingency criterion," *IEEE Trans. Power Syst.*, vol. 30, no. 6, pp. 3063–3071, Nov. 2015.

[20] P. A. Ruiz, J. M. Foster, A. Rudkevich, and M. C. Caramanis, "On fast transmission topology control heuristics," in *Proc. IEEE PES Gen. Meeting*, Detroit, MI, July 2011.

[21] J. D. Fuller, R. Ramasra, and A. Cha, "Fast heuristics for transmission-line switching," *IEEE Trans. Power Syst.*, vol. 27, no. 3, pp. 1377–1386, Aug. 2012.

[22] M. Soroush and J. D. Fuller, "Accuracies of optimal transmission switching heuristics based on DCOPF and ACOPF," *IEEE Trans. Power Syst.*, vol. 29, no. 2, pp. 924–932, Mar. 2014.

[23] M. Sahraei-Ardakani, A. Korad, K. W. Hedman, P. Lipka, and S. Oren, "Performance of ac and dc based transmission switching heuristics on a large-scale Polish system," in *Proc. IEEE PES Gen. Meeting*, National Harbor, MD, July 2014.

[24] E. A. Goldis, X. Li, M. C. Caramanis, C. R. Philbrick, A. M. Rudkevich, and P. A. Ruiz, "AC-based Topology Control Algorithms (TCA) a PJM historical data case study," in *Proc. 48th Hawaii Int. Conf. System Sciences*, Kauai, HI, Jan. 2015, pp. 2516–2519.

[25] P. A. Ruiz, A. M. Rudkevich, M. C. Caramanis, E. A. Goldis, E. Ntakou, and C. R. Philbrick, "Reduced MIP formulation for transmission topology control," in *Proc. 50th Allerton Conf. on Communications, Control and Computing*, Monticello, IL, Oct. 2012, pp. 1073–1079.

[26] E. A. Goldis, M. C. Caramanis, C. R. Philbrick, A. M. Rudkevich, and P. A. Ruiz, "Security-constrained MIP formulation of topology control using loss-adjusted shift factors," in *Proc. 47th Hawaii Int. Conf. System Sciences*, Big Island, HI, Jan. 2014.

[27] T. Güler and G. Gross, "Detection of island formation and identification of causal factors under multiple line outages," *IEEE Trans. Power Syst.*, vol. 22, no. 2, pp. 505–513, May 2007.

[28] T. Güler, G. Gross, and M. Liu, "Generalized line outage distribution factors," *IEEE Trans. Power Syst.*, vol. 22, no. 2, pp. 879–881, May 2007.

[29] PJM Markets and Operations. PJM Interconnection. Accessed Jan 20, 2016. [Online]. Available: http://http://www.pjm.com/markets-and-operations.aspx

[30] F. Schweppe, M. Caramanis, R. Tabors, and R. Bohn, *Spot Pricing of Electricity*. Norwell, MA: Kluwer, 1988.

[31] M. A. Lane, "Circuit breaker reliability & maintenance," in *Workshop on Transmission Topology Control*, Norristown, PA, Nov. 2013. [Online]. Available: http://www.pjm.com/ /media/committees-groups/stakeholder-meetings/transmission-topology-control/20131119-item-05b-lane-circuit-breaker-reliability-and-maintenance.ashx

[32] A. M. Rudkevich, "A nodal capacity market for co-optimization of generation and transmission expansion," in *Proc. 50th Allerton Conf. on Communications, Control and Computing*, Monticello, IL, Oct. 2012, pp. 1080–1088.

Pablo A. Ruiz (S'05, M'09) received the degree of Ingeniero Electricista (2002) from Universidad Tecnolgica Nacional-Santa Fe, Argentina, and the M.Sc. (2005) and Ph.D. (2008) degrees from the University of Illinois at Urbana-Champaign. He is Research Associate Professor of Mechanical Engineering at Boston University, Senior Associate in the Utilities Practice Area at The Brattle Group and Co-Founder, President and Chief Technology Officer at NewGrid, Inc. He was previously with AREVA T&D and Charles River Associates. His research is in power and gas systems and markets, including optimization, computations, economics, operations, and planning.

Evgeniy Goldis(S'12) received his B.S. from Harvey Mudd College in 2004 and his M.A. (2007) and Ph.D. (2015) from Boston University. His research interests include electricity and natural gas market design and optimization, as well as high-performance and cloud computing. He is currently the Chief Technology Officer of Newton Energy Group (NEG) and a senior consultant with TCR.

Aleksandr Rudkevich (M'09) received his M.Sc (1978). from the Gubkin Russian State University of Oil and Gas, Moscow, Russia and his Ph.D. (1988) from the Melentiev Energy Systems Institute of the Russian Academy of Sciences, Irkutsk, Russia. He is President and Co-Founder of Newton Energy Group with over 30 years of experience in energy economics, regulatory policy, and quantitative analyses of market fundamentals for electric power, natural gas and crude oil production and supply. His specialties include complex modeling of energy systems with applications to energy asset valuation, price forecasting, regulatory policy and market design.

Michael C. Caramanis (M'79) received his B.S. (1971) degree from Stanford University and his M.S. (1972) and Ph.D. (1976) from Harvard University. He is a Boston University Professor of Mechanical and Systems Engineering. Prof. Caramanis chaired the Greek Regulatory Authority for Energy and the International Energy Charters Investment Group (20014-2008), was personally involved in power market implementations in England (1989-90) and Italy (2000-03), and his written work has influenced Power Market design in the US and Europe. His current application domain focus is marginal costing and dynamic pricing on smart power grids, grid topology control for congestion mitigation, and the extension of power markets to include distribution connected loads, generation, and resources. He is coauthor of Spot Pricing of Electricity, Kluwer, 1987, and more than 100 refereed publications. His disciplinary background is in Mathematical Economics, Optimization, and Stochastic Dynamic Decision Making.

C. Russ Philbrick (M'99, SM'09) received his B.S. from Duke University in 1983 and his M.S. (1994) and Ph.D. (1997) from Stanford University. Through Polaris Systems Optimization, he develops tools to support power-grid reliability, efficiency and integration of renewable energy. Prior roles include Principle Power Systems Engineer (ALSTOM Grid 1999 to 2010), Associate Professor (Washington State University and Albrook Hydraulics Lab 1997 to 1999) and Submarine Officer (U.S. Navy 1984 to 2012). His experience includes nuclear plant operations and industrial engineering, and fields of interest include operations research, business process analysis, economics, probabilistic methods, and optimization. He has developed security-constrained unit commitment and economic dispatch tools broadly used by power markets and utilities.

Justin M. Foster (S09) received the BA. degree in mathematics from Bowdoin College, Brunswick, ME, in 2003, and the M.S. (2011) and Ph.D. (2012) degrees in systems engineering from Boston University, Boston, MA. He is currently Senior Trader and Principal with Appian Way Energy Partners, Cambridge, MA. He was previously with Edison Mission Marketing & Trading, Boston, MA.